ELSEVIER

Engineering Structures 23 (2001) 537–547

ENGINEERING STRUCTURES

www.elsevier.com/locate/engstruct

Seismic performance of RC frames designed for three different ductility levels

Yong Lu [a,*], Hong Hao [a], P.G. Carydis [b], H. Mouzakis [b]

[a] *School of Civil and Structural Engineering, Nanyang Technological University, Nanyang Avenue, Singapore 639798*
[b] *Laboratory for Earthquake Engineering, National Technical University of Athens, Athens 157-73, Greece*

Received 30 July 1999; received in revised form 8 March 2000; accepted 8 May 2000

Abstract

The concept of "making structures ductile" has prevailed in modern earthquake-resistant building design. In this context, questions remain regarding the selection of adequate ductility levels and the corresponding seismic force reduction factor q for a specific class of structures, whereas the detailing requirements to ensure the desired ductility continue to be refined. In the current investigation, three simple frames were designed for different ductility levels according to EC8 [Eurocode 8: Design provisions for earthquake resistance of structures. CEN (European Commission for Standardisation)/TC250/SC8, 1994] and their actual performance when subjected to earthquake simulation tests are observed and compared. Results indicate that under the "ductility for seismic force reduction" trade-off scheme, the frame designed for high ductility (thus large q factor) tends to attract more extensive damage due to large yield excursion, resulting in certain performance reduction. Insufficient confinement could lead to degrade hysteretic behaviour in a rather sensitive manner. Satisfactory performance was observed in the frame designed for medium ductility where both the seismic force reduction factor and the overall ductility were in the order of 3–4. In general, the overall and local ductility demands and the q-factors were observed to correlate in a rather predictable manner.

Keywords: Ductile design; Seismic force reduction; Hysteretic behaviour

1. Introduction

1.1. Conceptual background

Modern seismic codes of practice have adopted the concept that certain structural damage can be tolerated during major earthquakes, provided that structures are adequately ductile so that the inelastic energy dissipation can be achieved in a somewhat regulated manner without jeopardising the integrity or stability of the structural system. As a trade-off, the design seismic force can be drastically reduced, and this renders the ductile design be generally economical. However, ductility does imply damage, thus care must be exercised dealing with the following issues: (a) What ductility level may be regarded as adequate for a certain class of structures; (b) How much reduction of the design seismic force may be adequate for the ductility given; and (c) What particular design measures must be taken to ensure the desired ductility.

Answers to these questions are viable regardless what design approach (whether force based or displacement-based) is followed. However, simple solutions may not be possible owing to the wide diversity of structure forms and the large number of uncertainties involved. Nevertheless, at a conceptual level, some simplified relationships do exist and typical examples are seen in Fig. 1. Two idealised conditions define the boundaries for the relationship between the force reduction factor, q, and the overall ductility, μ_d:

(a) $\mu_d = q$ equal displacement approximation (1)

and

(b) $\mu_d = \frac{1}{2}(q^2+1)$ equal energy approximation. (2)

Structural systems with relatively long natural periods

* Corresponding author. Tel.: +65 7906914/7905278; fax: +65 7910676.
E-mail address: cylu@ntu.edu.sg (Y. Lu).

0141-0296/01/$ - see front matter
PII: S0141-0296(00)00058-4

(a) Seismic force reduction and ductility terms

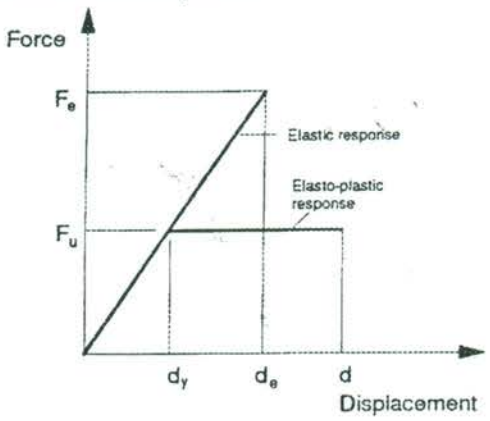

$q = F_e/F_u$

$\mu = d/d_y$

(b) Relationships between q-factor and ductility for idealised systems

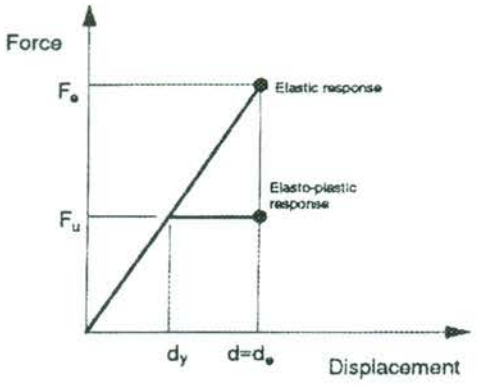

Equal displacement approximation: structures with relatively long natural period

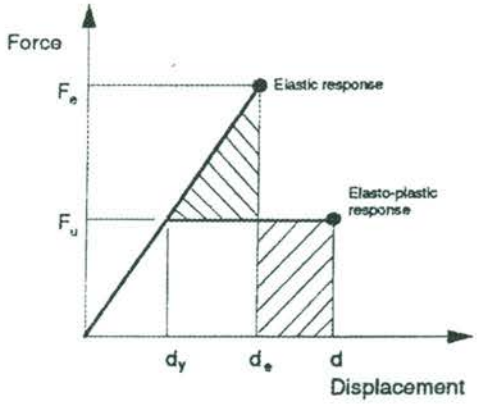

Equal energy approximation: structures with average natural period

Fig. 1. Conceptual relationships between seismic force reduction factor and ductility demands.

are likely to fall in the "equal displacement" category, whereas for those of average period the "equal energy" approximation is deemed more realistic.

In the Codes context, the demand on overall (displacement) ductility is brought further to relate with the curvature ductility at critical regions where most inelastic deformations take place. In this way, the quantified ductility demand is eventually connected to the design detailing requirements. One such attempt yields the following tentative expression concerning the critical curvature ductility demand ($\mu_{1/r}$) on columns [1]:

$$\mu_{1/r}=1+2(\mu_d-1). \quad (3)$$

For average frame systems, it is further simplified as [1]:

$$\mu_{1/r}=0.8q^2. \quad (4)$$

Expressions like the above appear to be attractive both for their conceptual soundness and simplicity. However, there has been lack of hard evidences as to what extent such simplified relationships may apply in actual structures subjected to earthquake excitations. This has been part of the motivations to the current investigation.

1.2. Explicit Code implementation: the EC8 approach and implications

The codes' translation of the loop of relationships described above is either explicit or in an implicit manner. The recent Eurocode 8 adopts an explicit approach and it can be schematically illustrated in Fig. 2. The implications may be that, whereas in general terms the overall "safety" against "collapse" is meant to be equal, the structures designed for different ductility classes are to have the following different performance characteristics:

1. Structures designed for ductility-class "High" (DC "High") tend to be most effective in economical terms

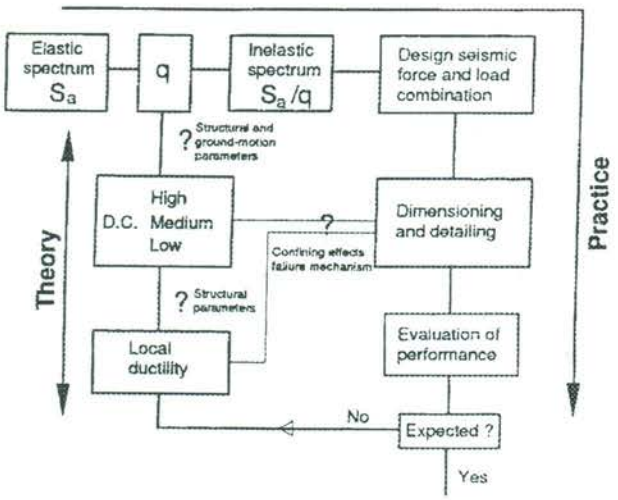

Fig. 2. Conceptual flowchart of the EC8 ductile design approach.

due to the largest reduction of the design seismic force (high q-value). The ductility enhancement measures should allow them to perform highly ductile under the prescribed earthquake intensity, whereas large inelastic excursions are expected to occur. As a result, the overall damage (including non-structural members) could be most extensive.

2. Structures designed for DC "Low" requires relatively high resistance (small q-factor) to counterbalance the low ductility supply. In return, their response would be of rather "stiff" nature with relatively small yield excursion under design earthquakes. However, vulnerability problem of "fragility" may arise in case of excessive ground motions.
3. Structures designed for DC "Medium" are expected to behave in an intermediate manner.

1.3. Objectives of the current research

As part of the efforts to assess the adequacy of the approach described above in structural design, and to add in the existing data base with experimental information particularly targeting the damage associated with a specific ductility level, three RC frames are investigated in this paper. These frames were designed for different ductility levels in accordance with the relevant provisions in EC8, and they were tested on an earthquake simulator with the following main objectives: (1) to compare the general seismic performance of these frames in all necessary terms, and to assess the detailing (confinement) requirements for the respective ductility; (2) to evaluate the actual ductility demands, the corresponding q-factors, and the actual damage associated with them; and (3) to provide some insights into the choice of an adequate design ductility level for simple RC frames.

2. Experimental program

2.1. Test structures

The main features of the three two-storeyed frames, designated as FH, FM and FML, respectively, are listed in Table 1. Namely, frames FH and FM were designed to conform with the EC8 design requirements for ductility class "high" and "medium" respectively, whereas frame FML was designed similar to frame FM except that the available local ductility (confining reinforcement) was purposely made lower than required to allow for a sensitivity observation. All the frames were designed for peak ground acceleration (PGA) of 0.30 g.

With regard to the general overstrength status of the designed frames, Table 1 also shows the design required base shear comparing to the predicted base shear strength taking into account the actual steel area and the characteristic material properties. The achieved maximum base shear strengths during testing are also listed for comparison. Apparently, an actual base-shear overstrength factor of approx. 2.5 was achieved in all three frames under investigation. This is considered normal as similar levels of overstrength have also been reported in many previous experimental investigations [2–5]. It is also noted that all frames herein were designed to satisfy the relevant EC8 requirements for "strong column, weak beam" systems. However, this did not seem to work exactly as expected and some column hinges eventually occurred during the tests, as will be seen later in Fig. 7.

The test frames were constructed at about 0.6:1 scale. Fig. 3 shows the dimensions of the frames and the typical reinforcement arrangement. The reinforcing details at the bottom regions of the columns [shown in Fig. 3(b)] highlighted the differences between these frames. The longitudinal reinforcement (8 mm dia.) had yield strength of 560 MPa and ultimate strength of approx. 650 MPa, its maximum elongation exceeded 20%. The yield strength of the transverse reinforcement (4mm dia.) was 455 MPa. The mean compressive strength of the concrete, measured on 100×200 mm cylinders, was 45 MPa.

2.2. Test setup and procedure

The test frames were mounted on the earthquake simulator by fixing the base girder on the simulator platform (Fig. 4). Due to reduced scale, the structural mass of the test frames had to be augmented so that the static normal stress as well as the stress induced by inertia forces in the model frame could be similar to that in the prototype frame [6]. These additional masses, accounting for 4000 kg per storey, were distributed and fixed on the floor slab by means of some prestressing devices.

Table 1
Main features and base shear strengths of test frames

	Frame "FH"	Frame "FM"	Frame "FML"
Design PGA	0.30 *g*	0.30 *g*	0.30 *g*
Ductility class	High	Medium	Medium
Design *q*-factor	4.5	3.0	3.0
Ductility supply	High	Medium	Low
Beam section (mm)	240×150	240×150	240×150
Column section (mm)	200×150	200×150	200×150
Critical column reinforcement per section	8D8S500	12D8S500	12D8S500
Critical column transverse steel	D4@30 mm	D4@40 mm	D4@55 mm
Design base shear	0.18 W (19.5 kN)	0.25 W (27.5 kN)	0.25 W (27.5 kN)
Predicted base shear strength[a]	0.35 W (38.5 kN)	0.47 W (51.5 kN)	0.47 W (51.5 kN)
Actual maximum base shear	0.47 W (52.0 kN)	0.59 W (64.9 kN)	0.57 W (62.5 kN)

[a] Using characteristic material strengths. "W" is the total weight of test structure.

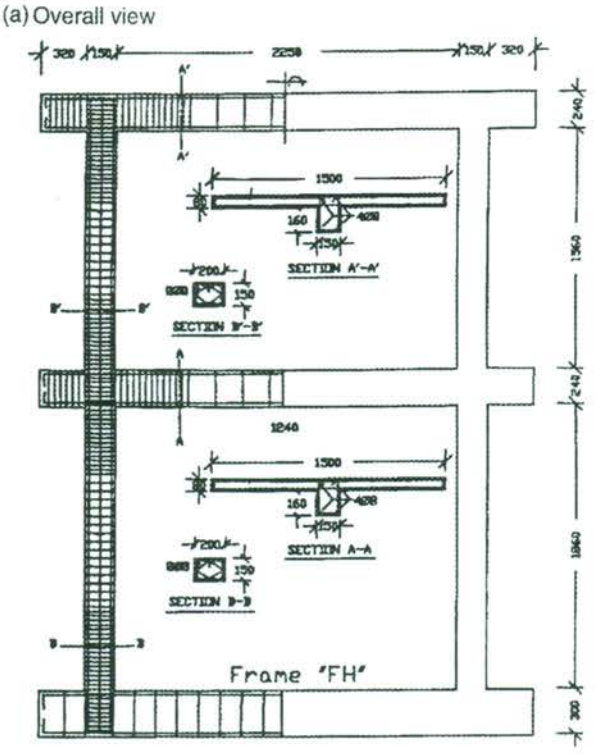

Fig. 3. Dimensions and reinforcement arrangement of test frames.

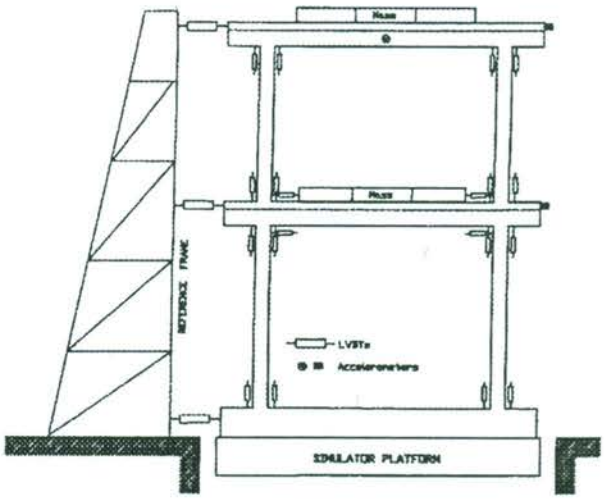

Fig. 4. Test set-up and instrumentation.

Besides, as each specimen was virtually a single piece plane frame, a side supporting system was installed to guide the test frame to respond within its plane.

The instrumentation, also shown in Fig. 4, was organised to measure the displacements and accelerations at all floor levels, as well as element end rotations for some beam and column members. Additional sensors were used to monitor the out-of-plane motion and the fixity of the base girders on the simulator platform.

The primary tests for each frame consisted of three consecutive horizontal earthquake simulations in the direction parallel to the frame plane, at increasing intensity. The input accelerograms were artificially generated to contain primarily a sine wave, with the amplitude of the acceleration being varied at the beginning and end of the waveform following a linear ramp, while the main portion of the accelerogram had a constant amplitude. The typical achieved base accelerations and the corresponding 5%-damped response spectra are shown in Fig.

5. As seen, in the first simulation test, the peak base acceleration was made equal to the corresponding design PGA (0.3 *g*). The second test had a peak base acceleration twice the design PGA. For the third test, the base acceleration amplitude was kept the same as for the second test, while the principal frequency of the accelerogram was adjusted to approach the measured fundamental frequency of the test model following the second test (Table 2). The modification to the accelerogram was considered necessary for securing the achievement of ultimate response of the specimens within the maximum acceleration capacity of the shaking table. After all, since the natural frequency of the specimen had reduced significantly during the second test, no simple scale correlation of the motion intensity would be possible even if the frequency characteristics of the accelerogram remained unchanged (scaling the peak acceleration up instead).

Complementary random vibration tests were performed before and after each earthquake simulation to determine the change of the dynamic properties of the structure.

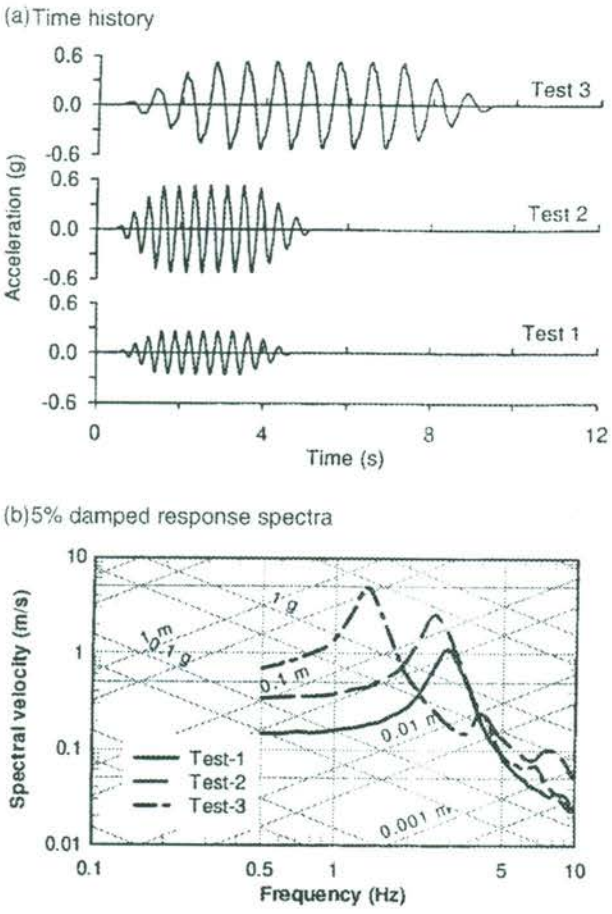

Fig. 5. Typical input accelerograms and corresponding response spectra.

2.3. Test results and discussion

2.3.1. Overall response

Fig. 6 illustrates the envelope relations between the measured base-shear (inferred from the inertia forces) and the first-storey drift for the three test frames.

As expected, the lowest base-shear resistance of frame FH (Ductility "High") resulted in a marked increase in the displacement response as well as the final ductility demand as compared to the other two frames. For those two frames, FM and FML, the base shear strengths were observed to approach each other despite the differences in the critical column confining reinforcement, and subsequently, the maximum displacements were about the same. These results clearly demonstrate a close relationship between the actual base shear strength and the maximum displacement or the ductility demand.

The extent of damage to the test frames was observed to closely relate to the displacement response. From the final cracking patterns depicted in Fig. 7, it is seen that frame FH experienced most extensive and spread damage. Inspection on local regions revealed severe spalling of concrete and visible buckling of the longitudinal reinforcement at the bottom regions of columns, while the maximum storey drift reached 6.0%. This signifies that the criterion concerning material failure, which constitutes one of the "collapse" criteria set forth in EC8, was eventually met in this particular frame at the above drift level. Comparatively, frame FM underwent less extensive damage, due apparently to the decreased displacement response (maximum drift less than 5%) while the available ductility seemed to be sufficient. Apparent sign of material failure was not observed. For frame FML, however, the performance was not as good although the maximum drift was at about the same 5% level. Crushing of concrete was observed to penetrate into core area while buckling of longitudinal reinforcement occurred at the bottom region of the columns. This could be attributed to the lack of sufficient confining effects in a quite sensitive manner in this particular frame. All frames exhibited much less server damage in the second storey than in the first.

2.3.2. Hysteretic relations

To further examine the ductile behaviour of the test frames, Fig. 8 illustrates the hysteretic relations between the measured base-shear and the first storey drift.

As can be seen from the hysteretic loops, all frames behaved similarly during low to moderate responses (Tests 1 and 2, the first and second batch of loops in the figure). Differences in hysteretic behaviour became apparent during advanced inelastic response (Test 3, the largest cycles), and they tend to show a close relationship with the extent of actual yield excursion and the available ductility. In the case of frame FH, large hystertic energy was observed, and yet at the maximum dis-

Table 2
Variation of measured frequencies of test frames and corresponding spectral response

Frame	Test No.	PGA (*g*)	Natural frequency (Hz)	Spectral response (elastic)	
				Acceleration (*g*)	Displacement (m)
FH	1	0.3	3.28	1.62	0.038
	2	0.6	2.23	2.26	0.113
	3	0.6	1.56	2.79	0.285
FM	1	0.3	3.29	1.57	0.036
	2	0.6	2.36	2.71	0.121
	3	0.6	1.62	2.40	0.227
FML	1	0.3	3.19	1.76	0.043
	2	0.6	2.27	2.33	0.113
	3	0.6	1.63	2.35	0.220

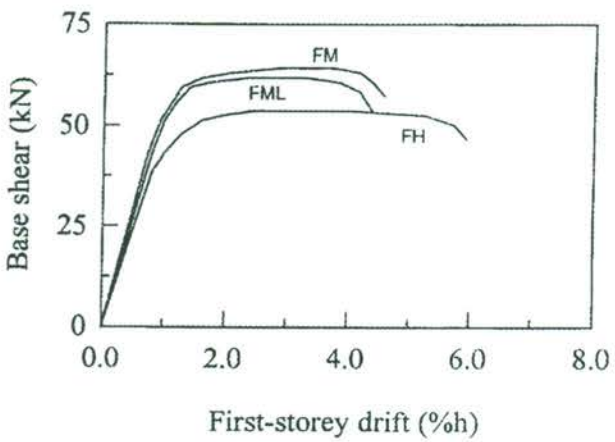

Fig. 6. Measured base shear vs displacement envelopes.

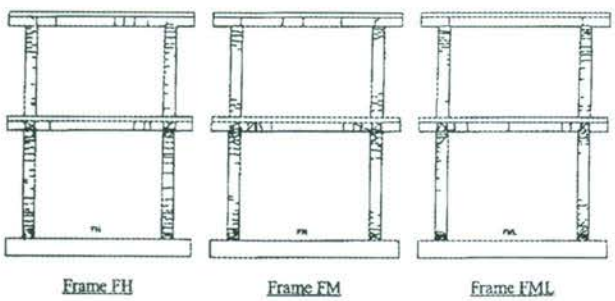

Fig. 7. Final cracking patterns of test frames.

placement it appeared to have reached the onset of hysteretic instability and the strength degraded for more than 20% during the second largest cycle. Frame FM again exhibited more satisfactory behaviour, with stable hysteretic loops running through a number of large cycles. On the other hand, the hysteretic response of frame FML was not as good, and in particular, a rather pronounced pinching occurred. This is consistent with the previous observation of insufficient confining reinforcement leading to crushing into core concrete during the maximum response.

2.3.3. Hystertic energy and equivalent damping

The hysteretic energy dissipation capacity is an important parameter quantifying the seismic performance of a ductile frame structure. In the context of the emerging displacement based design, the quantification of the hysteretic energy and the equivalent damping coefficient is a crucial step leading to the strength requirement for a target displacement under specific design earthquakes [7]. The current experiment provided some necessary information from which the hysteretic damping could be estimated and compared for frames with varying available ductility.

As can be seen from Fig. 8, for each tested frame two levels of inelastic response were achieved during test 2 and 3, respectively, and at each level several loading cycles were imposed. Therefore, the total hysteretic energy for the first three largest cycles (where available) can be computed and the average value is taken to represent the hysteretic energy per cycle at the specific response level for that particular frame. The equivalent hysteretic damping coefficient, ξ_e, is then calculated according to the following formula:

$$\xi_e = \frac{E_{hys}}{4\pi E_{el}} \tag{5}$$

where E_{hys} and E_{el} are the hysteretic and elastic strain energy of the system at a given displacement respectively. The hysteretic damping coefficients so obtained for the three frames herein are plotted versus the displacement ductility in Fig. 9. As seen, at the same displacement level (5% drift), frame FM exhibited 20% higher hysteretic damping than frame FML due to higher available ductility. In general, however, the differences are not very significant among the three frames under investigation, and an empirical relationship between the hysteretic damping coefficient (in percentage) and the displacement ductility demand may be written as follows:

$$\xi_e = \sqrt{100 - 6.25(\mu_d - 5)^2} \quad \text{for } \mu_d \leq 5 \tag{6}$$

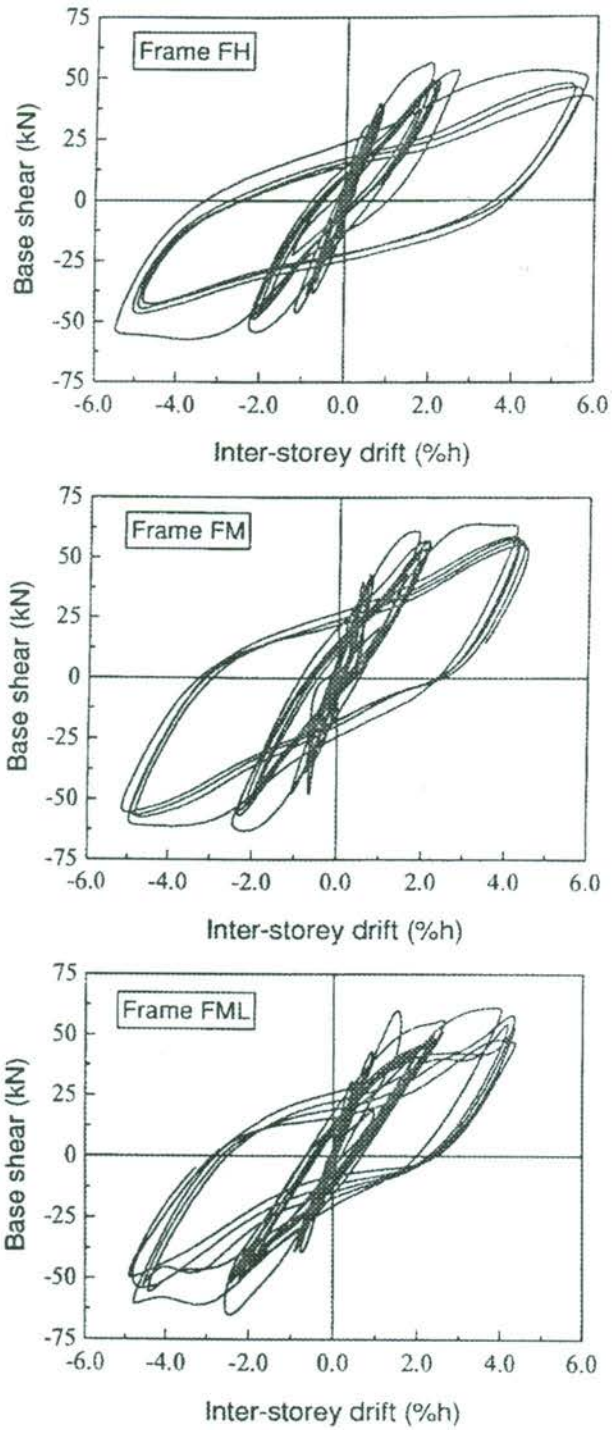

Fig. 8. Measured base shear vs displacement hysteretic relations.

2.4. Overall and local ductility demands and their inter-relationship

To estimate the ductility demand at a certain level of response requires first the determination of the yield

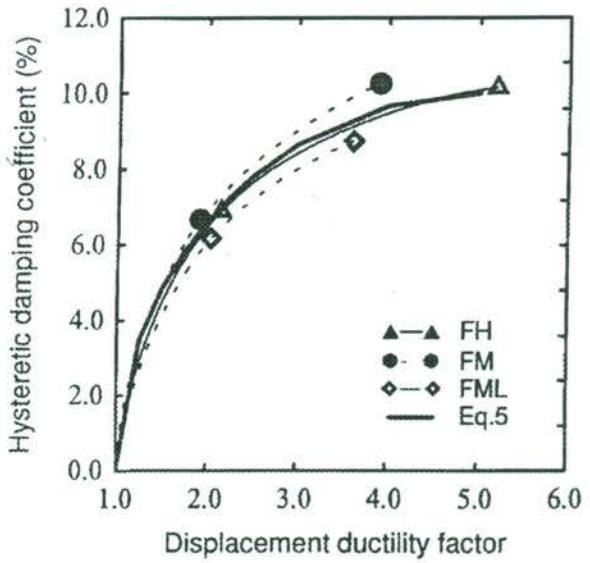

Fig. 9. Equivalent hysteretic damping coefficient vs displacement ductility.

deformation. Typical RC structures and elements are elasto-plastic systems which usually do not possess a well-defined yield point. For this reason, several alternatives have been proposed to represent the yield displacement for such systems [8]. In the present evaluation, the method depicted in Fig. 10 is employed to determine the yield displacement from the force–displacement response. Subsequently, the ductility demand is calculated as the ratio between the maximum displacement and the above yield displacement. The results show that the displacement ductility demands during the final tests were 5.2, 3.9 and 3.6 for frames FH, FM and FML, respectively.

The curvature ductility demands at critical column bottom regions were obtained from the moment–curvature relationship in a similar way. The moments in the column members were not directly measured though, instead, they were obtained on the basis of an inelastic analysis as described in the next section, and adjusted to be "experimental" by matching the computed and the measured base shear. The measured curvature, on the other hand, was obtained from the measured column end rotation divided by the corresponding gauge length (equal to the cross-section depth herein). The resultant curvature ductility demands for the final tests were found to be 8.1, 6.1 and 6.5 for frames FH, FM and FML, respectively.

As can be seen, similar to the displacement ductility demands, the required curvature ductility for frame FH was about 30% higher than that for frame FM. It is interesting to note that the required curvature ductility for frame FML was higher than that for frame FM (6.5 vs 6.1) although its displacement ductility demand was somewhat smaller (3.6 vs 3.9). This is believed to be a

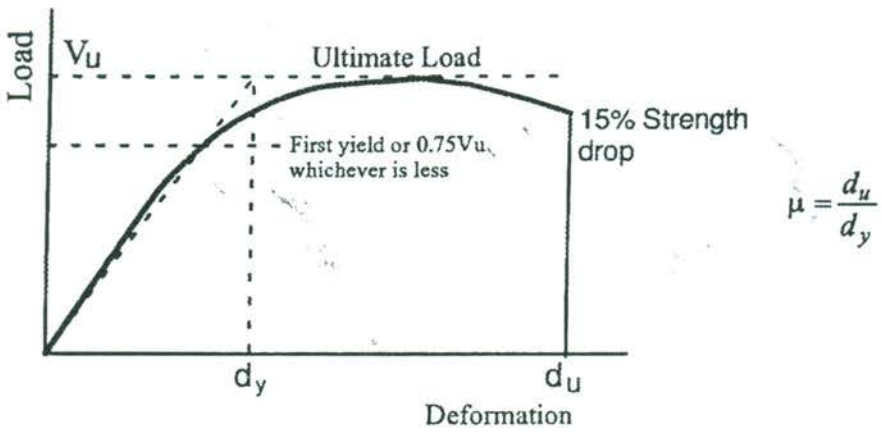

Fig. 10. Estimation of ductility factor for elasto-plastic systems.

result of severer concentration of the local damage in frame FML, as described earlier.

Fig. 11 plots the relationship between the displacement and curvature ductility demands for the three particular frames herein, at two response levels (Tests 2 and 3). The tendency resembles quite well the approximation given by Eq. (3).

2.5. Evaluation of q-factor and its relationship with ductility demands

For the test frames, the seismic force reduction factor q at any inelastic test stage (Test 3, for example) can be calculated as the ratio between a "would-be" elastic base shear response, V_e', along the line of the representative elastic stiffness, and the actually measured base shear strength, V_u:

$$q=\frac{V_e'}{V_u}. \tag{7}$$

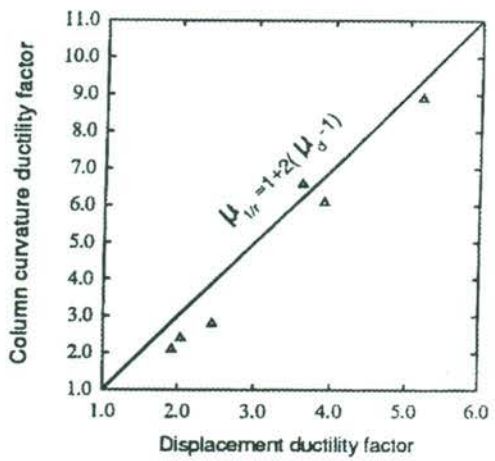

Fig. 11. Relationship between measured displacement ductility and critical column ductility factors.

The quantification of V_e would be a simple matter of extrapolating the base shear measured during an elastic test (Test 1) if the relative intensity of the inelastic base motion on the elastic system could be known. In actual testing, however, the natural frequencies of the specimen vary from test to test as a result of cumulative damage, therefore, no simple scale correlation between base motion intensities seems to be possible even if the same accelerogram is used throughout the tests. A possible way to quantify the intensity of varying accelerograms is to adopt the "spectrum intensity" approach [9], but again the variation of the natural frequency of the structure is not properly accounted for. In what follows, an "equivalent spectral response" concept is adopted to derive the aforementioned "would-be" elastic base shear response corresponding to an inelastic test.

Assuming the fundamental period of the specimen at a representative elastic stage is T_0, and it is increased to T_1 immediately before the inelastic test of interest, due to decrease of stiffness from K_0 to K_1. For period T_1, the spectral acceleration, velocity and displacement of the particular inelastic base motion are S_{a1}, S_{v1} and S_{d1} respectively (refer to Fig. 5). The maintenance of equivalent effects of this base motion on the elastic system implies all the above spectral quantities to remain when this base motion is imposed on the elastic system. Apparently, this would not be possible unless the elastic system is "tuned" to have the same period as the inelastic structure. Whereas the elastic stiffness K_0 has to remain to represent the elastic system, the above "tuning" can only be achieved by adding hypothetic mass to the system so that:

$$T_0'=\sqrt{m_0'/K_0}=T_1=\sqrt{m_1/K_1} \tag{8}$$

where T_0', m_0' are the period and effective mass of the "tuned" elastic system, and T_1, m_1, K_1 are the period, effective mass and stiffness of the actual inelastic struc-

ture, respectively, m_1 can be approximated by the elastic effective mass m_0. Recasting Eq. (8) yields:

$$m_0' = m_1 K_0 / K_1 = m_0 (T_1/T_0)^2 \tag{9}$$

where T_0 is the period of the elastic system.

Now that the stiffness of the above "tuned" system is the same as of the elastic state, subjecting this system to the inelastic base motion yields the "would-be" elastic base shear as follows:

$$V_c' = m_0' S_{a,1} = m_0 \left(\frac{T_1}{T_0}\right)^2 S_{a,1} = \left(\frac{T_1}{T_0}\right)^2 m_0 S_{a,0} \frac{S_{a,1}}{S_{a,0}} \tag{10}$$

$$= \left(\frac{T_1}{T_0}\right)^2 \frac{S_{a,1}}{S_{a,0}} V_0$$

where $V_0 = m_0 S_{a,0}$ is the measured base shear during the elastic test for which the spectral acceleration is $S_{a,0}$. Eq. (10) can also be written in spectral displacement terms as:

$$V_c' = \frac{S_{d,1}}{S_{d,0}} V_0 \tag{11}$$

From here it can be seen that the estimation of the "would-be" elastic base shear is indeed an extrapolation process with however the spectral displacement response as a measure of relative intensity. Note that the spectral displacement has the same dimension as the "spectrum intensity" mentioned earlier. Referring to the spectral response data summarised in Table 2, the q-factors were thus calculated to be 4.5, 3.6 and 3.7 for frame FH, FM and FML respectively for the final tests.

A summary of the q-factor and the corresponding overall and local ductility estimates is given in Fig. 12, in which the inter-relationships between these factors are plotted and compared with those given by Eqs. (3), (4) and (6). As can be seen, the "observed" q-factor vs displacement ductility relationship herein more closely resembles the "equal displacement" approximation. On the other hand, the simplified relationship between the q-factor and the local ductility, given by Eq. (6), is shown to have a large margin of safety for the particular frames under investigation [Fig. 12(b)]. Similar observations were also obtained in some previous investigations involving multi-storey frame structures [10].

2.6. Analysis of frame response using global modelling technique

As mentioned in the previous section, a numerical analysis was incorporated in the investigation to assist the interpretation of the experimental results. As a side product, this also enabled a calibration of using the global beam–column modelling scheme for frame analysis into advanced inelastic response. Although recent developments in computing technique have enabled wider application of sophisticated finite element models for inelastic analysis of RC structures, problems with RC material modelling still hampers the effective use of such models in the dynamic analysis of complex structures and particularly with advanced inelastic response. For this reason, an adequate use of the classical beam–column modelling for frame analysis is still of great interests.

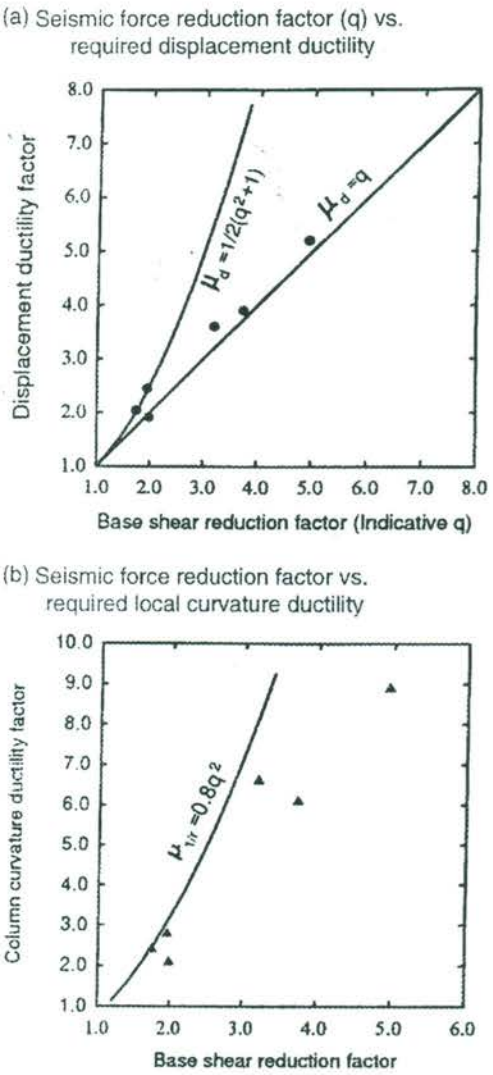

Fig. 12. Comparison of measured and simplified relationships between seismic force reduction factor and required overall/local ductility.

Fig. 13 shows the frame model and the restoring force pattern used in the current analysis. The restoring force model is a modified version of the Takeda model, taking into account the stiffness degradation. The computer code is originated from program DRAIN2-D [11]. A 3% viscous damping coefficient was considered. It is worth mentioning here that choice of a realistic starting stiffness for each individual analysis was found to affect the

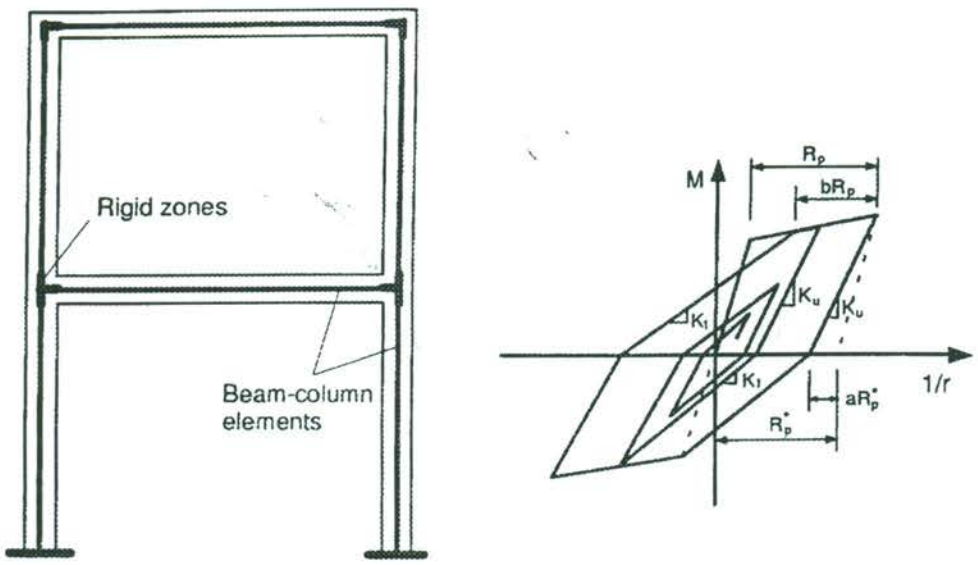

Fig. 13. Global frame model and corresponding restoring force pattern.

accuracy of the inelastic response prediction. In this analysis, the actual decrease of the overall stiffness, as reflected from the variation of the measured natural frequencies, was considered for each simulation calculation.

Fig. 14 shows the comparison between the computed and measured displacement time histories for frame FH subjected to base motions measured during Tests 2 and 3, as well as the corresponding hysteretic loops. The comparison for the remaining two frames was similar to the situation presented here.

As can be seen, both time history and hysteretic response predictions show a good agreement with the measured response. This confirms that the beam–column modelling scheme can be successfully used in inelastic frame analysis concerning response at both global and elemental levels. The output of such analysis can also be used to supply loading histories for isolated critical regions to facilitate a reduced scale FE analysis for response at the material level.

3. Conclusions

Based on the results described in this paper, the following conclusions may be drawn:

1. The amount of confining reinforcement at the critical regions of columns improved the local behaviour as well as the overall ductility of frames in a rather sensitive manner; improvement of the hysteretic behaviour (including the hysteretic damping) was also evident as a result of adequate confinement. The EC8 detailing requirements regarding critical confining reinforcement as applied in these test frames seem to be justified;
2. Under the "ductility for seismic force reduction" trade-off scheme, the experimental observations suggest that frames designed for high ductility (thus large reduction of design seismic force) are likely to attract more extensive damage than those designed for lower ductility, due to large yield excursion. In the context of a performance based design rather than merely for non-collapse or life-safety concerns, this would increase the difficulty for the high ductility class designs to meet specific displacement performance criteria. Comparatively, the medium ductility design (Frame FM), for which the design q-factor and overall ductility requirement were both in the order of 3–4, demonstrated most satisfactory performance with reduced overall damage and a good hysteretic behaviour under a comparable base motion. Of course, for a given ductility class design, efforts to gain enhanced ductility within the same economical constraint should always be encouraged.
3. For the simple frames considered, the observed relationship between the displacement ductility and the local (column) curvature ductility resembles well a simplified linear relationship which is given by Eq. (5). The observed relationship between the seismic force reduction factor q and the ductility demands tend to agree with the equal displacement approximation, i.e. $q=\mu_d$. As regards a direct estimation of the local curvature ductility demand from a given q-

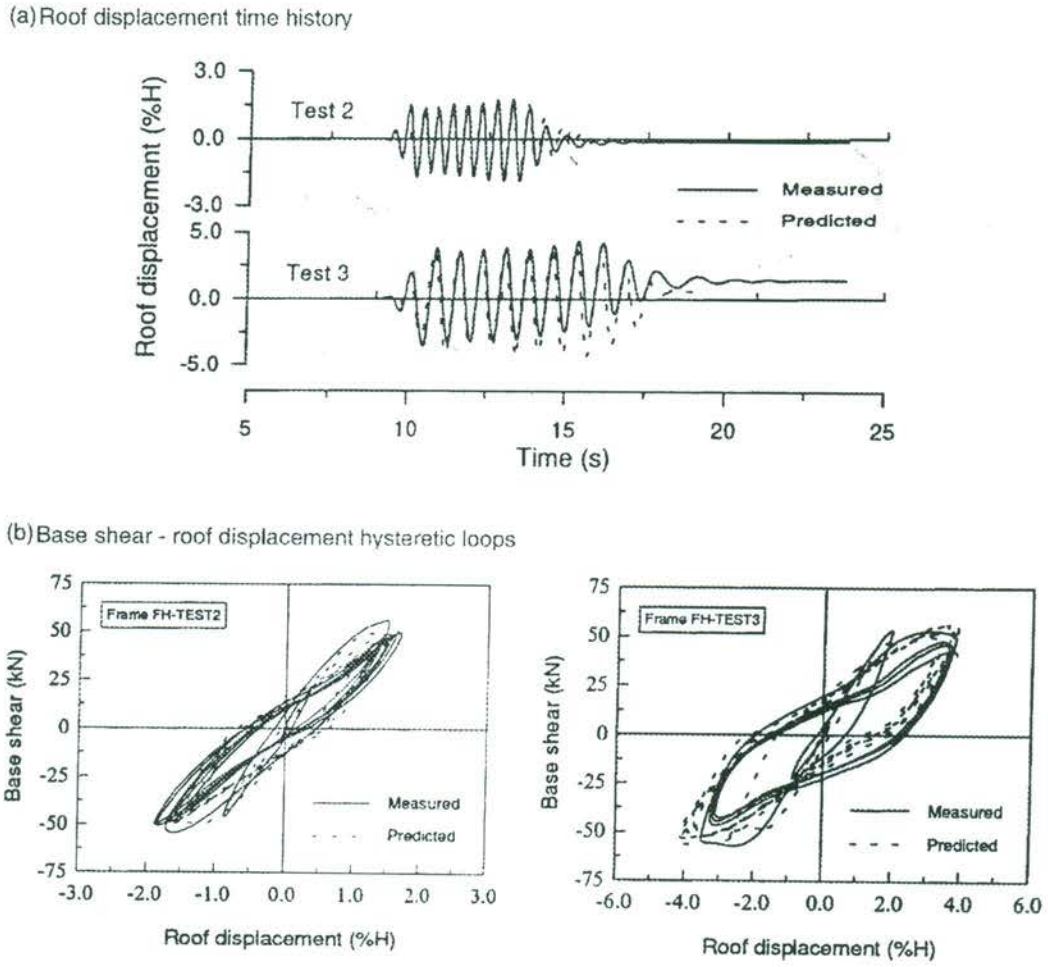

Fig. 14. Comparison between measured and computed responses of frame FH.

factor, Eq. (6) is found to have a large margin of safety for the particular frames herein.

References

[1] "Justification Notes", EC8 Background Documents Part II, prepared by T. P. Tassios, Athens, Greece, 1988.
[2] Charney FA, Bertero VV. An evaluation of the design and analytical seismic response of a seven-storey reinforced concrete frame-wall structure. Report No. UCB/EERC-82-08. Earthquake Engineering Research Centre, University of Berkeley, CA, 1982.
[3] Moehle JP, Sozen MA. Experiments to study earthquake response of R/C structures with stiffness interruptions. Civil Engineering Studies, Structural Research Series No. 482, Uniersity of Illinois, Urbana, IL, 1980.
[4] Shahrooz BM, Moehle JP. Seismic performance and design of setback buildings. Journal of Structural Engineering, ASCE 1990;116(5):1423–39.
[5] Lu Y, Tassios TP, Zhang GF, Vintzileou E. Seismic response of reinforced concrete frames with strength and stiffness irregularities. ACI Structural Journal 1999;96(2):221–39.
[6] Tassios TP. Model analysis of RC structures subjected to seismic or cyclic loading. In: Noor FA, editor. Small Scale Modelling of Concrete Structures. Oxford: Elsevier Applied Science, 1993.
[7] Priestley MJN. Performance based seismic design. Proc., 12WCEE, (Paper ID: 2831), Auckland, New Zealand, 2000.
[8] Park R. Evaluation of ductility of structures and structural assemblages from laboratory testing. Bulletin of the New Zealand National Society for Earthquake Engineering 1989;22(3):155–66.
[9] Housner GW. Strong ground motion. In: Wiegel RL, editor. Earthquake engineering, Englewood Cliffs, NJ: Prentice-Hall, 1970:75–92.
[10] Lu, Y. Study of seismic behaviour of reinforced concrete frames having vertical irregularities. Ph.D. thesis presented to the National Technical University of Athens, Greece, in partial fulfilment of the requirements for the degree of doctor of engineering, 1996.
[11] Kanaan AE, Powell GH. DRAIN-2D: a general purpose computer program for dynamic analysis of inelastic plane structures. Report No. UCB/EERC-73/6, Earthquake Engineering Research Centre, University of Berkeley, CA, 1973.